

UC San Diego

UC San Diego Previously Published Works

Title

Issues with centrifuge modelling of energy piles in soft clays

Permalink

<https://escholarship.org/uc/item/3tp9q4r7>

ISBN

978-1-138-34422-8

Authors

Ghaaowd, I
McCartney, J
Huang, X
[et al.](#)

Publication Date

2018-07-11

DOI

10.1201/9780429438646-95

Peer reviewed

Issues with Centrifuge Modeling of Energy Piles in Soft Clays

I. Ghaaowd, Doctoral Candidate

J. McCartney, Associate Professor

University of California San Diego, La Jolla, California, USA

X. Huang, Ph.D. Student

Hohai University, Gulou Qu, Nanjing Shi, Jiangsu Sheng, China

F. Saboya, Professor

S. Tibana, Associate Professor

ABSTRACT: This study focuses on an experimental evaluation of issues encountered when using a geotechnical centrifuge to evaluate the heat transfer, pore water pressure generation, volume change, and subsequent soil-structure interaction phenomena associated with energy pile operation in normally-consolidated Kaolinite clay. Although the scaled zones of influence of heat transfer and volume change due to thermal consolidation in centrifuge models may be wider than those expected in a field-scale prototype, centrifuge modeling results can still be used to validate numerical simulations performed at model scale. Further, topics such as the impact of temperature changes on the ultimate capacity of energy piles are well-suited to centrifuge testing due to the difficulty of performing such tests in the field. The energy pile investigated in this study is an aluminum cylinder whose temperature is controlled using an embedded electrical resistance heater. This paper focuses on an evaluation of the transient response of a soft clay layer during heating and cooling of the energy pile, an evaluation of the change in undrained shear strength profiles measured using a T-bar, and a comparison of the pullout capacity of the heated energy pile with that of an unheated energy pile.

1. INTRODUCTION

When a heat source such as an energy pile is embedded in a saturated clay layer, temperature changes will result in changes in pore water pressure as the rate of heating is typically faster than the rate of drainage (Ghaaowd et al. 2016). Although all soils will initially expand during undrained heating, normally consolidated soils typically exhibit permanent contraction while overconsolidated soils exhibit expansion after sustained heating (Vega & McCartney 2015). Subsequent cooling typically leads to elastic contraction. Thermally-induced changes in pore water pressure and volume may affect the soil-structure interaction of energy piles, as well as the ultimate capacity of the energy pile.

There have been several previous studies that have emphasized the importance of considering the effects of temperature changes on the behavior of soils and associated effects on embedded structural elements like energy piles. Booker & Savvidou (1985) proposed analytical solution to predict the temperature change and thermal excess pore water pressure as a function of distance from a cylindrical heat source in a thermo-elastic soil layer. Savvidou (1988) found that centrifuge modeling of thermo-mechanical processes in soils requires consideration of thermal convection effects, and that lower permeability soils are less affected by convection.

Ghaaowd et al. (2016) developed and validated a model to predict the change in pore water pressure of saturated clay as a function of depth in a soil layer during undrained heating based on the model of Campanella & Mitchell (1968). Their model indicates that the initial mean effective plays a critical role in the magnitude of pore water pressure change during undrained heating, which implies that centrifuge testing has an advantage over 1g testing in that the effective stresses are similar to those in a prototype soil layer. Takai et al. (2016) found that thermally-induced pore water pressures during undrained heating cannot be used to predict the volume change observed during drained heating, although they may be related. Maddocks & Savvidou (1984) studied the heat transfer from a hot cylinder installed in soft clay in a centrifuge test and observed changes in thermal excess pore water pressure and time-dependent contraction as a function of distance from the cylinder. Stewart & McCartney (2013) studied the soil-structure interaction in an end-bearing energy pile in unsaturated silt and found that the heat transfer does not scale, resulting in a greater zone of influence of temperature changes. They found that the centrifuge still can provide useful information on soil-structure interaction phenomena and recommended use of model-scale results in validation of numerical models. Ng et al. (2014) used a centrifuge to study the effects of cyclic heating of an aluminum energy

pile in soft clay and observed permanent settlement that accumulated with each cycle. McCartney & Murphy (2017) evaluated the long-term response of a full-scale energy pile in claystone during building heat pump operation and observed a transient change in the thermal axial strains over a period of five years that was attributed to dragdown that may arise from the effect of temperature.

This study investigates the behavior of a normally-consolidated Kaolinite clay layer during heating and cooling of an embedded aluminum energy pile. The Actidyn C61-3 centrifuge at the University of California San Diego was used to perform two tests on energy piles in separate soil layers, the first in which an energy pile was installed using jacked-in procedures, heated to a constant temperature, cooled, then pulled out at a constant rate after reaching equilibrium, and the second where the energy pile was installed similarly then pulled out at a constant rate after reaching equilibrium without heating. The results for the heated energy pile include the variations in temperature and pore water pressure generation in the clay layer, the undrained shear strength profile, as well as the pullout capacity for heated and unheated energy piles are also compared. For brevity, the soil-structure interaction evaluation involving assessment of thermal axial strain profiles and potential dragdown effects are not presented in this paper.

2. MATERIALS

2.1. Kaolinite Clay

The soil used in the two experiments was commercially-available Kaolinite clay from M&M Clays Inc. of McIntyre, Georgia whose geotechnical properties of the clay are summarized in Table 1. The clay classifies as CL according to the Unified Soil Classification Scheme. An isotropic compression test indicates that the slopes of the normal compression line (λ) and the recompression line (κ) for the clay are 0.100 and 0.016, respectively. The clay specimens were formed from a slurry to reach initially normally consolidated conditions as will be described below.

Table 1. Properties of the Kaolinite clay and initial conditions of the specimen used in this study.

Liquid limit	47%
Plastic limit	28%
Plasticity index	19
Specific gravity	2.6

2.2. Scale-Model Energy pile

The scale-model energy pile is a 25 mm-diameter, 255 mm-long, split-shell aluminum cylinder having a wall thickness of 3.3 mm, as shown in Figure 1. At 50 g, the model pile corresponds to a prototype pile having a diameter of 1.25 m and a length of 12.75 m. The insides of the cylinder halves were instrumented with five temperature-compensated strain gages and thermocouples at the locations shown in Figure 2. The halves are held together by screw-on top and bottom caps. An internal electrical resistance heater running the length of the energy pile is connected to the top cap, and heat is conducted from the heater to the outside of the pile through a sand fill. The top cap of the pile was fabricated from plastic to minimize heating of the water ponded on the soil surface, and all wiring passes through the top cap.

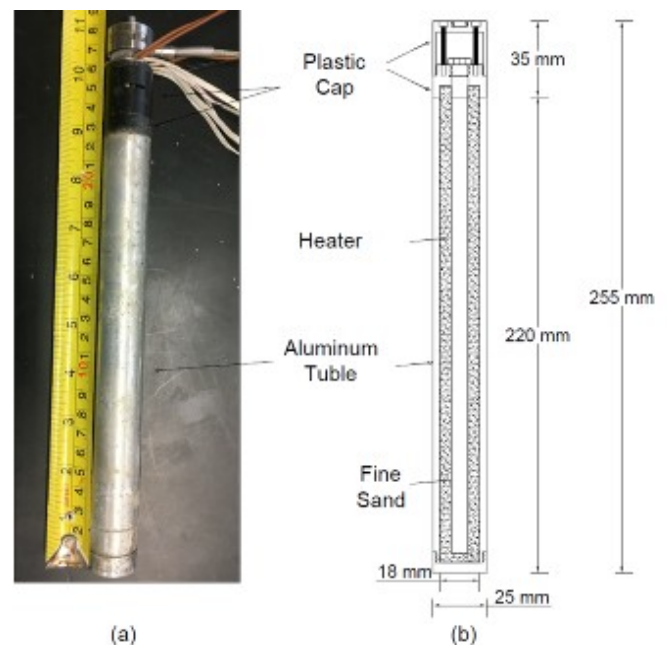


Figure 1. (a) Assembled energy pile, (b) Pile cross section with model-scale dimensions.

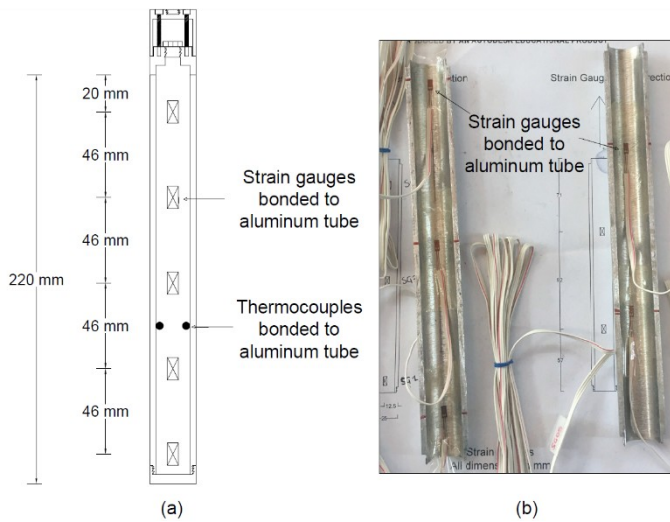


Figure 2. (a) Schematic showing the model-scale locations of strain gauges, (b) Picture of strain gauges bonded to the aluminum tube.

3. EXPERIMENTAL SETUP

A schematic of the container used in this study to evaluate the behavior of an energy pile in normally consolidated clay is shown in Figure 3. The aluminum container consists of a base plate, a cylindrical tank, and an upper reaction plate. The base and reaction plates of the container have dimensions of 0.62 m×0.62 m×0.05 m. The cylindrical tank has an inside diameter of 0.55 m, a wall thickness of 16 mm, and a height of 0.47 m, and was connected to the base plate via four threaded rods atop an “O”-ring seal. The top reaction plate was connected to the top ends of the same threaded rods. The reaction plate supports stepper motors for loading the energy pile and T-bar, as well as displacement sensors.

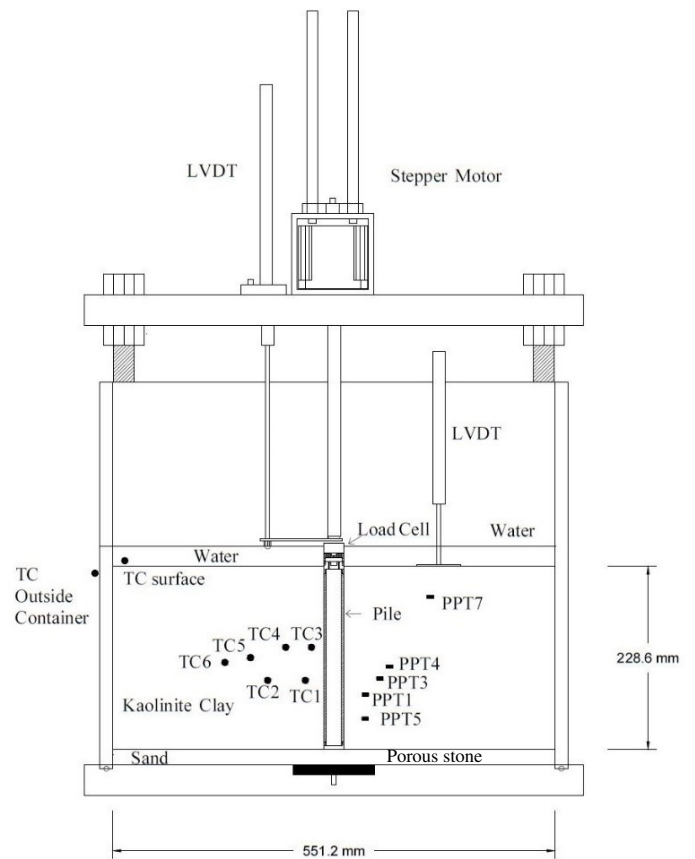


Figure 3. Cross-section of the test setup showing the energy pile, T-bar, thermocouples, and pore water pressure sensors.

The energy piles were installed in flight through sedimented clay layers having a thickness of 228 mm so that they would bear on a dense sand layer to simulate end-bearing boundary conditions. A stepper motor was used to insert the pile at a constant-displacement rate to simulate jacked-in conditions. The motor movement is controlled using a LabVIEW program capable of applying both constant-displacement conditions as well as constant axial head loads (i.e., to simulate the dead weight of an overlying structure). The applied axial head load was measured using a load cell. Six thermocouples and five miniature pore water pressure sensors were inserted through the container side wall into the clay layer at the locations shown in Figure 3 and Table 2.

A T-bar with a diameter of 14 mm and length of 57 mm was used to measure the undrained shear strength profiles of the clay layers containing heated and unheated energy piles. The T-bar was designed to permit model-scale penetrations up to 230 mm and was driven by a second stepper motor at a model-scale velocity of 0.2 mm/s to ensure undrained conditions during insertion and extraction. Insertion of the T-bar into the clay layer can be used to infer the undrained shear strength of the intact clay layer as a function of depth, while extraction of the T-bar can be used to infer the undrained shear

strength of disturbed clay as a function of depth (Stewart and Randolph 1994).

Table 2. Sensor locations with respect to the container center and soil surface

Transducer	Depth (mm)	Radius (mm)	Sensor	Depth (mm)	Radius (mm)
PPT1	160	36	TC1	142	36
PPT3	140	85	TC2	142	83
PPT4	125	53	TC3	108	28
PPT5	190	66	TC4	102	60
PPT7	38	116	TC6	121	136

4. EXPERIMENTAL PROCEDURES

The kaolinite clay in powder form was mixed with water in a vacuum mixer to reach a slurry having a gravimetric water content of 130%. The slurry was carefully poured into the container to avoid air inclusions. The clay specimen was drained from the bottom via a sand layer having a thickness of 20 mm thickness and from the top via a filter paper and a 50 mm-thick porous stone placed on the top of the slurry. After 24 hours of self-weight consolidation, dead-weights applying vertical stresses of 2.4, 6.3, 10.2 kPa were added in 24-hour increments. The surcharge was then increased to 23.6 kPa using a hydraulic piston and maintained for another 24 hours. Then the container was placed inside the centrifuge basket for in-flight self-weight consolidation at 50 g. This procedure was found to produce a normally-consolidated clay layer with an overconsolidated portion at its top, and is similar to the approach proposed by Cinicioglu et al. (2006).

During in-flight self-weight consolidation at 50 g, the excess pore-water pressures were monitored using five pore pressure transducers. An example of the excess pore water pressure measured by pore water pressure transducer (PPT4) is plotted against the square root of time in Figure 4. This data permits definition of the value of t_{90} using the root time method (Taylor 1948). The measured pore water pressure at the end of the consolidation was compared with the theoretical hydrostatic pore water pressure profile in Figure 5. These results confirm that primary consolidation was reached throughout the clay layer. The gravimetric water content of the clay layer with the unheated pile measured at the end of testing ranged from 38.5 to 52%, while the void ratio ranged from 1.0 to 1.35. These values can be assumed to correspond to the

initial conditions for the energy pile before the heating and cooling cycle.

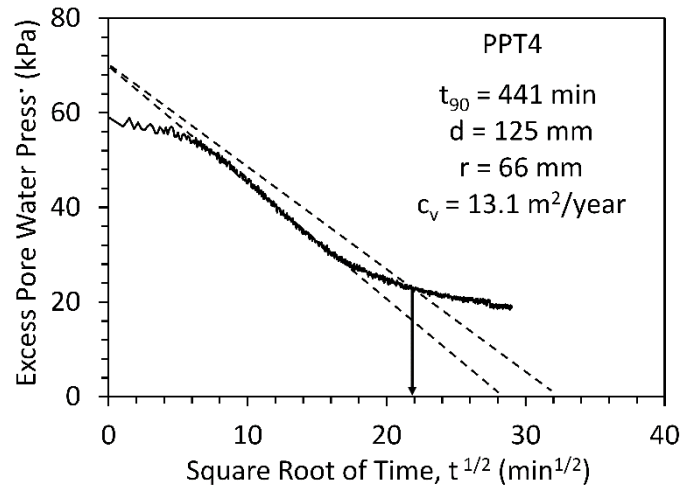


Figure 4. Excess pore water pressure measured by PPT4 versus the square root of time

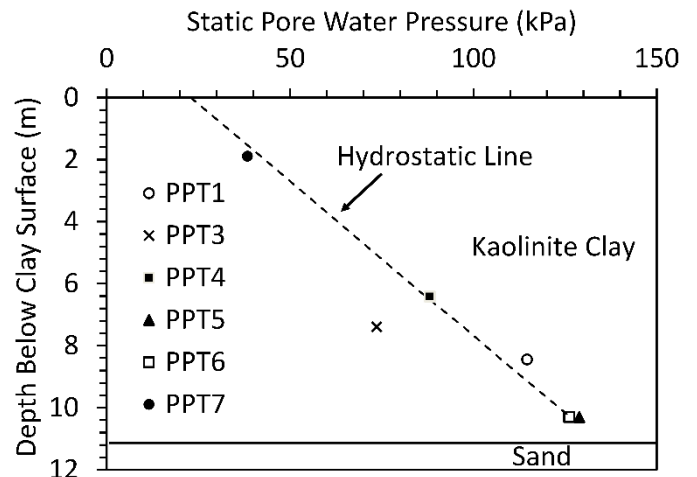


Figure 5 Pore water pressure profile after consolidation with depth in prototype-scale.

After consolidation, the pile was inserted into the clay at a model-scale velocity of 0.1 mm/s until the tip reached the sand layer. The pile was inserted so that the aluminum portion was embedded in the clay and the plastic top cap was above the clay surface, with a prototype-scale embedment of approximately 11 m. The pile was loaded to a prototype-scale compressive load of 1445 kN, which is expected to mobilize most of the side shear resistance and mobilization of the end bearing. A control loop was used to maintain the load under constant-load conditions (i.e., free displacement conditions). When the excess pore water pressure generated due to the pile insertion was dissipated, the temperature of the heated energy pile was increased using the Watlow heat controller until reaching a maximum temperature at the pile wall of 63.4 °C. Heating continued for 31 hours during centrifugation to

permit stabilization of both temperature and pore water pressure. As the strains scale 1:1 in the centrifuge, the thermal expansion strains are expected to be the same in the model and prototype. After heating, the pile was cooled and was then pulled out at the same insertion speed used for installation. T-bar tests were executed in each test at a radius of 100 mm from the heated and unheated energy piles, which is far enough away to be undisturbed from the pile insertion and extraction but close enough to be influenced by temperature.

5. EXPERIMENTAL RESULTS

5.1. Temperature response

Time series of the pile and clay temperatures at different locations are shown in Figure 6, and the temperature changes versus radius at various times are shown in Figure 7. The pile temperature increased very quickly due to the rapid response of the electrical resistance heater, but the temperature of the clay increased gradually and stabilized after 10 hours in model scale (1041 days in prototype scale). Although the heater in the pile increased in temperature from 26.0 to 63.4 °C ($\Delta T = 37.4$ °C), the soil only reached a maximum temperature change of 15.9 °C. The temperature decreased away from the energy pile with a negligible change at the container boundary of 276 mm. When the electrical resistance heater was turned off, the clay temperature rapidly decreased to a temperature of 30 °C. This is greater than the initial temperature, perhaps because the heat pulse was still moving through the clay layer and because the temperature of the centrifuge chamber increased to nearly 29 °C in during the 50 hours of centrifuge heating.

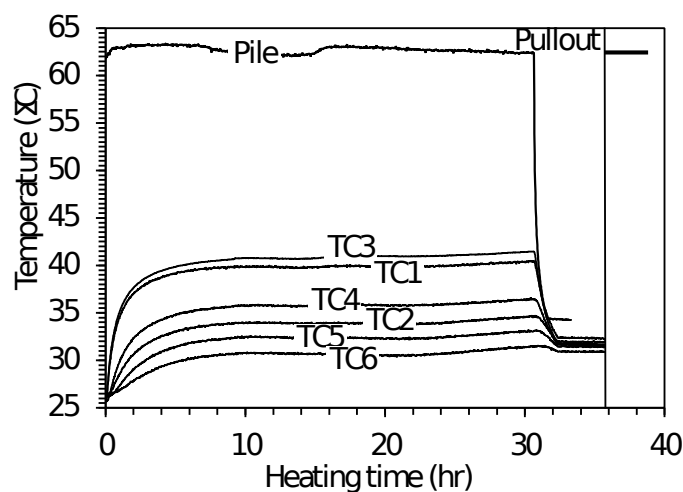


Figure. 6 Temperature versus heating time at different radii

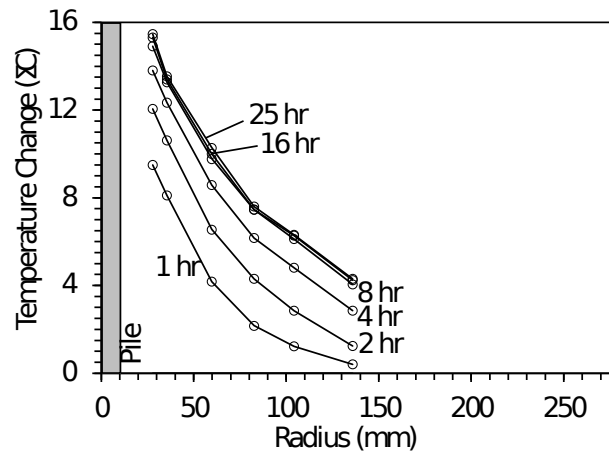


Figure 7. Temperature changes at different heating times.

5.2. Thermal excess pore water pressure

Thermal excess pore water pressures were generated in the clay immediately after the increase in temperature, as shown in Figure 8. This increase in pore water pressure occurs due to partially undrained conditions and the difference between the coefficients of thermal expansion of the clay solid skeleton and the water (e.g., Ghaaowd et al. 2015). The pore water pressures immediately started to dissipate, with thermal consolidation finishing after approximately 21 hours. Although the data acquisition unit used for the pore water pressure sensors in this test had some noise issues that have since been rectified, the dissipation trends in the data are clear. PPT7 shows an initial increase in pore water pressure followed by a dissipation that goes below zero, which could be due to issues with the sensor or slight changes in the surface water level due to evaporation induced by the elevated soil temperature. The maximum measured thermal excess pore water pressure was 18.2 kPa at PPT1, due to the combination of the depth of the sensor and the greater temperature change at this location. The thermally induced excess pore water pressure did not fully dissipate at this location by the end of heating, although they likely returned to static values after cooling.

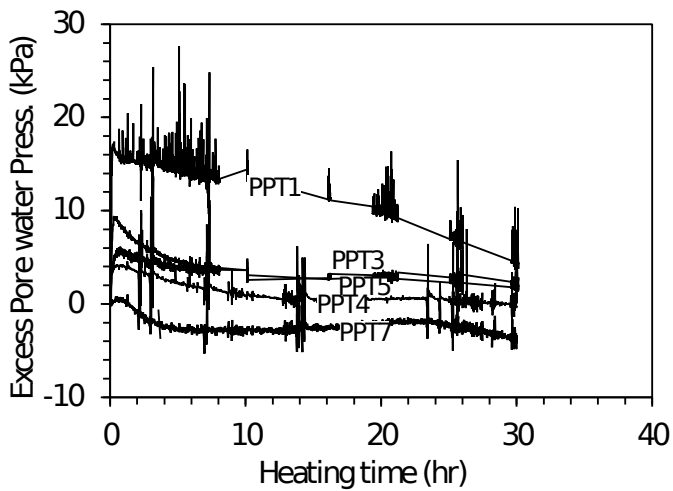


Figure 8. Thermal excess pore water pressure versus heating time at different radii and different depths

The change in pore water pressure at the effective stress associated with the prototype depth of PPT1 predicted by the model of Ghaaowd et al. 2015) is 17 kPa, so the measured value is reasonable. Similar checks were performed for the other sensors, and the predicted and measured maximum excess pore water pressure are shown in Figure 9. In general, most of the predicted pore water pressures were above those measured by the sensors. Differences in the predicted and measured values may be due to changes in vertical position of the PPTs due to consolidation, transient changes in temperature at the different locations, and the different distances from the drainage boundaries that may result in partial drainage of the thermal excess pore water pressures.

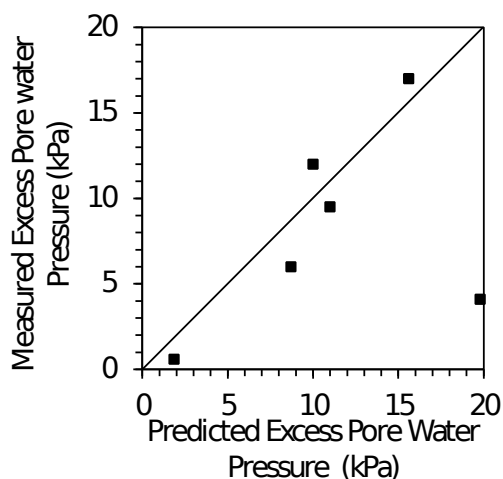


Figure 9. Measured excess pore water pressure versus predicted pore water pressure from the model of Ghaaowd et al. (2015).

6. T-BAR MEASUREMENTS AND INTERPRETATION

The T-bar measurements in the clay layers with heated and unheated energy piles provide further evidence as to the effects of heating and cooling on the temperature effects on the behavior of normally consolidated clay layers. The correlations of Stewart & Randolph (1991) were used to interpret the undrained shear strength profiles from the T-bar measurements. The undrained shear strength profiles for the clay layer at a model-scale distance of 100 mm from the unheated and heated energy piles are shown in Figure 10. The undrained shear strength profiles indicate that heating of the energy pile leads to an increase in undrained shear strength of the clay layer during both insertion and extraction. Greater differences in undrained shear strength were observed deeper in the clay layer, which may be because the thermally induced excess pore water pressures were greater at these depths. The initial T-bar position is slightly below the clay surface to maximize the stroke of the T-bar test, so the undrained shear strength near the surface of the clay layer may not be well characterized.

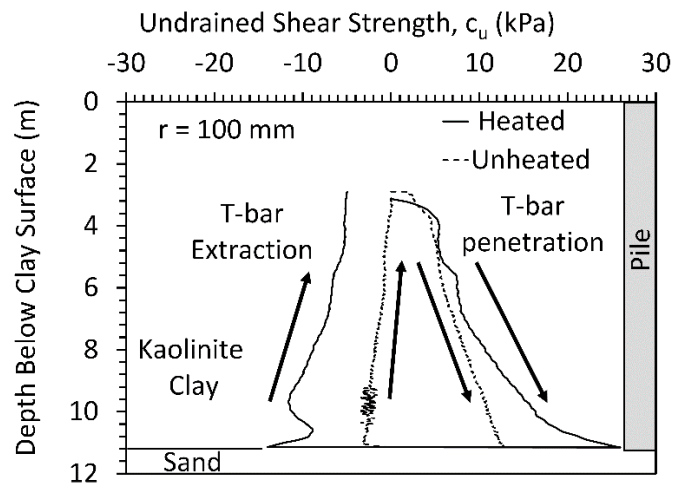


Figure 10. Undrained shear strength measured by T-bar (positive values for insertion and negative values for extraction)

7. PULLOUT CAPACITY

The net pullout pile capacities for the heated and unheated energy piles in clay layers having similar initial conditions are shown in Figure 11, with respect to the initial compressive seating load of 1445 kN. The heated energy pile had a pullout capacity of -723 kN that is 20% greater than that of the unheated energy pile that had a pullout capacity of -370 kN. This significant increase in capacity confirms that the drained heating processes leads to

substantial improvements in the undrained shear strength of the soil surrounding the heated energy pile. The slopes of the pullout curves are similar, even though the aluminum energy pile experiences a significant axial strain in the direction opposite to loading during heating. This will be further investigated in the future using the axial strain measurements.

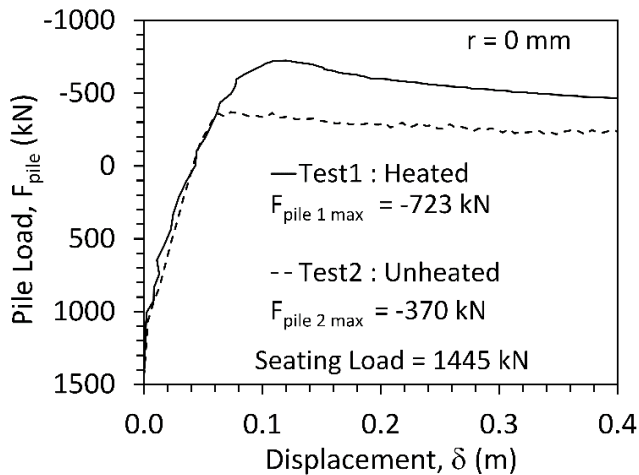


Figure 11. Pullout-displacement curves for heated and unheated energy piles in prototype scale

As a check on the measured capacity of the unheated energy pile, the pullout capacity was predicted using the equation of Dennis and Olson (1983):

$$Q_s = c_u \alpha A_s F_c F_L \quad (4)$$

where the c_u is the mean undrained shear strength measured using the T-bar, α is an empirical side shear reduction capacity factor (equal to 1 for the soft clay evaluated in this study), A_s is the pile surface area, F_c is a sampling correction factor (equal to 1.0), and F_L is a length correction factor (equal to 1.0). It is assumed that the pile has no negative end bearing. The predicted pullout capacity of the unheated energy pile is -362 kN, while the measured pullout capacity of the unheated pile is -370 kN.

8. CONCLUSION

Heated and unheated scale-model aluminum energy piles were tested to evaluate the impacts of temperature on the a normally consolidated clay layer and on the corresponding pullout capacity of

the energy pile. The following specific conclusions can be drawn:

- The temperature in the clay stabilized after 10 hours of heating, which led to relatively undrained heating of the clay layer. The pore water pressure gradually dissipated after this time.
- The temperature change and the vertical effective stress are directly proportional to the thermal excess pore water pressure generation.
- The measured undrained shear strength profiles at a model-scale radius of 100 mm both the tests on heated and not heated energy piles were interpreted using from T-bar tests. The undrained shear strength of the soil surrounding the heated-cooled energy pile was higher than the soil surrounding the unheated pile, with greater increases in undrained shear strength deeper in the soil layer.
- The pullout capacity of the heated energy pile was approximately 20% greater than that for the unheated energy pile, with a similar slope for the pullout curve.

REFERENCES

- Booker, J.R. & Savvidou, C. 1985. Consolidation around a point heat source. *International Journal for Numerical and Analytical Methods in Geomechanics*, (9): 173-184.
- Campanella, R.G. & Mitchell, J.K. 1968. Influence of temperature variations on soil behavior. *Journal of the Soil Mechanics and Foundation Division*. 94(SM3): 709-734.
- Cinicioglu, O., Znidarčić, D. & Ko, H.-Y. 2006. "A new centrifugal testing method: Descending gravity test." *Geotechnical Testing Journal*. 29(5): 1-10.
- Dennis, N.D., & Olson, R. E. 1983. Axial capacity of steel pipe piles in clay. *Proc., Conf. on Geotech. Pract. In Offshore Eng., S. G. Wright, ed., ASCE, New York: 370-388.*
- Ghaaowd, I., Takai, A., Katsumi, T. & McCartney, J.S. 2016. Pore water pressure prediction for undrained heating of soils. *Environmental Geotechnics*. 4(2): 70-78.
- McCartney, J.S. & Murphy, K.D. 2017. Investigation of potential dragdown/uplift effects on energy piles. *Geomechanics for Energy and the Environment*. 10(June): 21-28.
- Maddocks, D.V. & Savvidou, C. 1984. The effect of the heat Transfer from a hot penetrator installed in the ocean bed. *Proc. Symp. on the Application of Centrifuge Modeling to Geotechnical Design*. W.H. Craig, Manchester U.K
- Ng, C.W.W., Gunawan, A. & Laloui, L. 2014. Centrifuge modelling of energy piles subjected to heating and cooling cycles in clay. *Géotechnique Letters*, 4(4): 310-316.
- Savvidou, C. 1988. Centrifuge modelling of heat transfer in soil. *Proc. Centrifuge 88. Balkema: 583-591.*

- Stewart, D. & Randolph, M. 1994. T-Bar penetration testing in soft clay. *J. Geotech. Eng. Div.* 120(12): 2230-2235.
- Stewart, M.A. & McCartney, J.S. 2013. Centrifuge modeling of soil-structure interaction in energy foundations. *Journal of Geotechnical and Geoenvironmental Eng.* 04013044.
- Takai, A., Ghaaowd, I., Katsumi, T., & McCartney, J.S. 2016. Impact of drainage conditions on the thermal volume change of soft clay. *Proc. GeoChicago 2016*: 32-41.
- Taylor, D.W. 1948. *Fundamentals of Soil Mechanics*. John Wiley and Sons, New York.
- Vega, A. & McCartney, J.S. 2015. "Cyclic heating effects on thermal volume change of silt." *Environmental Geotechnics*. 2(5): 257-268.